INSTITUTE OF PHYSICS PUBLISHING SEMICONDUCTOR SCIENCE AND TECHNOLOGY

Semicond. Sci. Technol. **17** (2002) 898–906 PII: S0268-1242(02)37917-3

Heterojunction bipolar transistors implemented with GaInNAs materials

P M Asbeck[1], **R J Welty**[1], **C W Tu**[1], **H P Xin**[1] **and R E Welser**[2]

[1] University of California, San Diego La Jolla, CA 92093-0407, USA
[2] Kopin Corporation, 695 Myles Standish Boulevard, Taunton, MA 02780, USA

Received 26 February 2002
Published 17 July 2002
Online at stacks.iop.org/SST/17/898

Abstract

Use of GaInNAs in the base of heterojunction bipolar transistors (HBTs) on GaAs substrates allows a reduction of the turn-on voltage, $V_{\mathrm{be,on}}$, of the devices, facilitating their use in applications with low power supply voltage (particularly battery operated power amplifiers for mobile communications). Using GaInNAs with N content below 2% and In content of 1–20%, HBTs have been demonstrated with $V_{\mathrm{be,on}}$ values lower by 25–400 mV than those of conventional GaAs-based HBTs. The GaInNAs base regions exhibit lower diffusion length than conventional GaAs bases, which reduces current gain and detracts from high-frequency performance, as well as higher base sheet resistance. These adverse effects can be mitigated by proper design tradeoffs of base thickness and nitrogen composition, as well as by compositional grading in the base to provide a built-in quasi-electric field to assist electron transport.

1. Introduction

One of the devices that can be expected to benefit from the application of GaInNAs is the heterojunction bipolar transistor (HBT) implemented with GaAs substrates. GaAs HBTs are in widespread use, particularly in microwave power amplifiers for wireless applications. The use of GaInNAs in the base region of the HBTs allows the turn-on voltage, $V_{\mathrm{be,on}}$ applied between base and emitter to be adjusted in a way that improves HBT performance in battery-powered operation.

The structure of representative GaAs HBTs manufactured at present is shown in figure 1(*a*). With a substrate of semi-insulating GaAs, the devices comprise epitaxial layers corresponding to a collector of n-type GaAs, a base of p-type GaAs and an n-type emitter of a material whose bandgap is wider than that of the base (typically $\mathrm{Al}_x\mathrm{Ga}_{1-x}\mathrm{As}$ with $x \sim 0.25$ or GaInP). This is followed by a cap layer of GaAs or InGaAs to assist in forming the emitter ohmic contact. An associated band diagram is shown in figure 1(*b*). With the wide bandgap of the emitter, high emitter injection efficiency is maintained independent of the emitter and base doping levels, so that it is possible to achieve high current gain (>40 for microwave applications, >100 for digital and mixed-signal applications) even with very heavily doped base regions (with hole concentration in the range of $1–5 \times 10^{19}$ cm^{-3}). The transistors achieve very high microwave power gain because of the low base resistance and short base transit time. They also can achieve high values of breakdown voltage (>25 V $BV_{\mathrm{cbo}} > 15$ V BV_{ceo}) as required for robust operation in power amplifiers.

As a result of the advantages of the GaAs-based HBTs, they have become the devices of choice for the power amplifiers used in many cellular phone handsets, particularly those with high linearity requirements (for example, phones that follow the CDMA standard and use QPSK modulation). The manufacturing volume of the GaAs HBT amplifiers has reached 200 million units per year. Substantial attention has been paid to low cost production of 6 inch diameter wafers.

While the GaAs HBTs characteristics are closely matched to the needs of linear, efficient power amplifiers operated with available batteries, there are several features which could be improved. One of these is the turn-on voltage, $V_{\mathrm{be,on}}$, needed to produce current flow. For present GaAs-based HBTs, the value of $V_{\mathrm{be,on}}$ is of the order of 1.4 V (near the bandgap of the base). The power amplifier circuits are customarily operated using a battery as the voltage source, and Li ion cells are widely used at present. The voltage provided by these cells is in the neighbourhood of 3.4–3.6 V, but can drop to 3.0 V near the end of the battery discharge cycle (and rise to 4.2 V when fully charged). Circuit considerations require that $V_{\mathrm{be,on}}$ should be well below half the minimum battery hvoltage, in order to implement temperature-compensated bias circuitry in the

0268-1242/02/080898+09$30.00

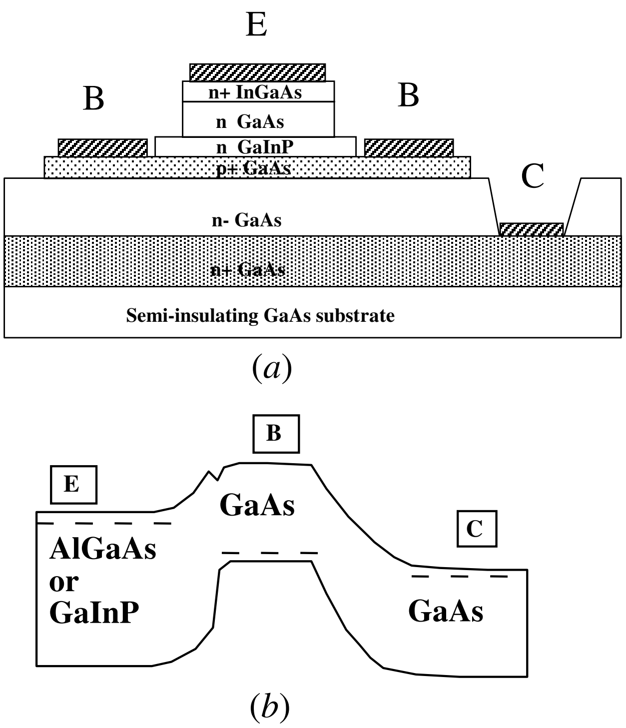

(*a*)

(*b*)

Figure 1. (*a*) Representative GaAs HBT layer structure; (*b*) corresponding HBT band diagram.

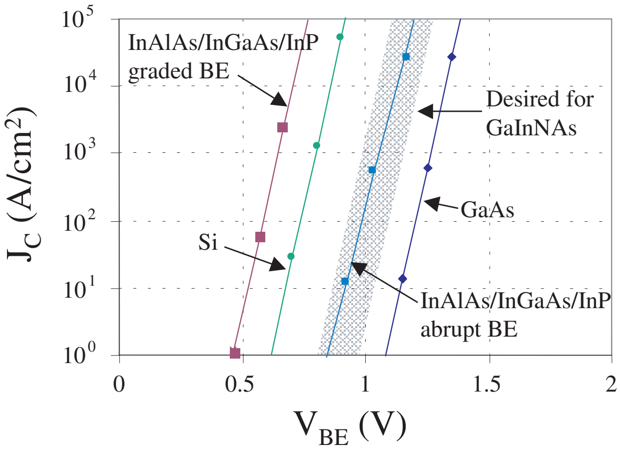

Figure 2. Representative variation of collector current density, J_{C}, versus V_{be} for HBTs fabricated with different material systems. The shaded region shows the values obtainable with HBTs using GaInNAs base regions.

amplifiers. The present value of $V_{\mathrm{be,on}}$ for HBTs is marginal for these requirements. As a result, there is substantial benefit that can be obtained by a relatively small decrease in $V_{\mathrm{be,on}}$.

For most HBTs employed at present, the output current is controlled by base transport rather than by heterojunction barriers at the base-emitter or base-collector junctions. Under such conditions, the value of V_{be} required to achieve a given collector current per unit emitter area, J_{C}, can be found from

$$V_{\mathrm{be}} = \frac{KT}{q}\ln\left(\frac{J_{\mathrm{C}}\int p/ni^2\,\mathrm{d}x}{qD_{\mathrm{n}}}\right). \tag{1}$$

The integral is taken across the quasi-neutral base region (of thickness w). V_{be} has a weak dependence on D_{n}, the diffusion coefficient for electrons in the base, on the hole concentration p in the base, and on the width of the base [13]. The principal determinant of V_{be}, however, is the intrinsic carrier concentration in the base, n_{i}, where

$$n_{\mathrm{i}}^2 = N_{\mathrm{C}}N_{\mathrm{V}}\exp\left(\frac{-E_{\mathrm{g}}}{kT}\right). \tag{2}$$

The value of n_{i} is largely controlled by the bandgap energy E_{g} of the material used in the base. Figure 2 illustrates the dependence of J_{C} on V_{be} found for a variety of HBTs fabricated with different material systems. The value of $V_{\mathrm{be,on}}$ is smaller in Si devices than in GaAs-based HBTs, and smaller yet in HBTs on InP substrates with lattice-matched $\mathrm{In_{0.53}Ga_{0.47}As}$ base regions. For various circuit applications, as mentioned, it is desirable to decrease the value of $V_{\mathrm{be,on}}$ by a small amount. The use of GaInNAs materials in the base can provide a technologically important small shift in bandgap, leading to I_{C} versus V_{be} dependence in the shaded region of figure 2. A principal goal of the research activities for GaInNAs-based devices is to demonstrate this reduction in $V_{\mathrm{be,on}}$ without compromising the high microwave performance of the transistors (including high current gain, low base resistance, low base transit time, high breakdown voltage, high current-gain cutoff frequency and high reliability). Research results suggest that the desired material characteristics can be obtained. It is additionally found that with the GaInNAs base regions there can be a reduction in the 'offset voltage' (the minimum value of V_{CE} when the device is on) which further improves the efficiency of the resulting amplifier circuits.

In this paper, first the design considerations for HBTs, based on GaInNAs are discussed. Then experimental demonstrations reported to date are reviewed. The prospects and limitations of the technology are subsequently summarized.

2. Design considerations for GaInNAs-based HBTs

The principal objective of GaInNAs-based HBT design is to replace the p-type GaAs base layer of figure 1 with a corresponding layer of GaInNAs that has a lower value of bandgap energy. The choice of alloy composition for the base is constrained by a number of factors. Lattice-match to the GaAs substrate must be relatively good, in order to avoid exceeding the critical thickness for misfit dislocation formation (which leads to excess recombination in the base). Representative thicknesses of the layers used in the HBT base are in the range 400–800 Å. These are substantially greater than the layer thicknesses used for quantum wells in laser applications [1–3], and correspondingly the requirements for lattice-match are more stringent for HBTs than for lasers. Using values for material parameters taken for GaAs, the estimated in-plane lattice strain versus $\mathrm{Ga}_{1-x}\mathrm{In}_x\mathrm{N}_y\mathrm{As}_{1-y}$ alloy composition is shown in figure 3. The tensile strain obtained by the addition of nitrogen compensates for the compressive strain obtained by In additions, in an amount approximately given by 1 mol% nitrogen to compensate 3 mol% In [3]. The amount of strain allowed for a critical thickness of 600 Å is estimated to be 0.37%, while for a thickness of 100 Å (typical of quantum well applications) it is estimated to be 1.4%. The associated lines on figure 3 illustrate representative bounds

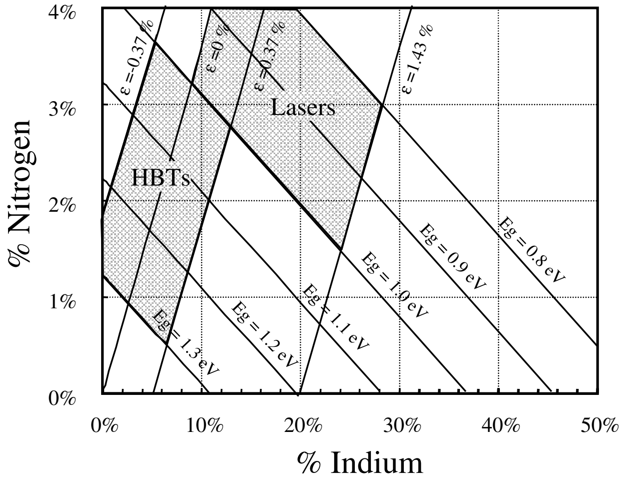

Figure 3. Schematic values of epitaxial layer strain ε and energy bandgap, as a function of alloy composition (indium and nitrogen) for GaInNAs on GaAs substrates.

for alloys of interest for the two applications. Figure 3 also shows contours for the estimated bandgap energy of the alloys, calculated from the approximate relation:

$$\mathrm{GaIn}_x\mathrm{N}_y\mathrm{As}\ E_\mathrm{g}(x, y) = 1.43 - 1.15x - 10.0y. \qquad (3)$$

This is based on linear interpolation of the bandgap reduction as a result of adding nitrogen [4] or indium [5]. In order to provide a useful amount of $V_{\mathrm{be,on}}$ reduction in HBTs, the bandgap of the GaInNAs in the base should be in the range 1.0–1.3 eV. By contrast, for lasers it is desirable to reduce the bandgap to 0.9 eV or below (to achieve 1.3 or 1.55 μm emission after quantum well confinement energy is accounted for). This constraint allows a further definition of the regions of interest for the different applications, which are shown as shaded areas in figure 3. The figure shows that the target compositions are substantially different for the two different devices; HBTs require substantially better lattice-match, but can succeed with more modest reductions in bandgap, than lasers. A wide range of material compositions have been explored in initial laboratory experiments, by a number of investigators. In general it is found that by using the lowest possible amount of nitrogen, the device characteristics are improved.

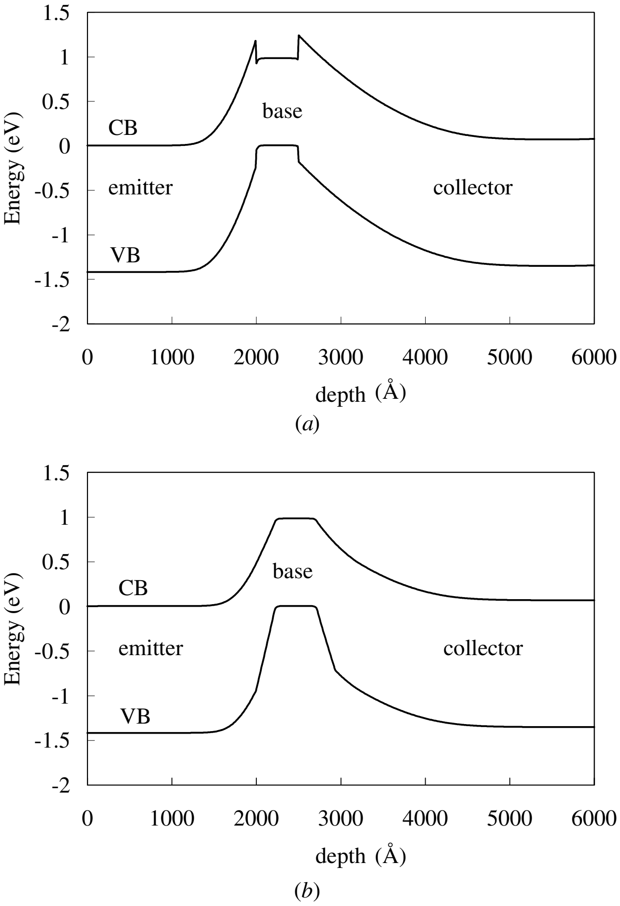

(*a*)

(*b*)

Figure 4. Band diagram of HBT with GaInNAs base where no provisions are made to reduce BE and BC conduction-band barriers. Also shown is the calculated band diagram for the design of table 1, which incorporate provisions to overcome conduction band barriers at the BE and BC heterojunctions.

It has been established that the majority of the change in bandgap energy of GaInNAs relative to GaAs occurs in the conduction band, rather than the valence band. This arrangement is relatively unfavourable for npn HBT applications (although, as detailed below, favourable for pnp devices) since the offset of conduction band, energy can produce an energy barrier for electrons at the GaAs/GaInNAs interface. Figure 4(*a*) shows a band diagram for a device that would result if special care is not given to mitigate the energy barriers. At the base-emitter junction, the presence of a barrier dictates that higher applied voltage must be used to inject electrons into the base, and so leads to an increase in $V_{\mathrm{be,on}}$ (negating the benefit of the GaInNAs base). At the base-collector junction, the effect of a conduction band barrier is even more significant, since it impedes collection of the minority carriers by the high-field collector region. This leads generally to a dramatic decrease in current gain and increase in charge storage in the base as well as to a reduction in collector current, which frequently becomes dependent on the base-collector reverse bias voltage. Research in other material systems (for example, InP/InGaAs/InP HBTs) has shown that a variety of techniques can be used to minimize the effects of the conduction band offset at the junctions. Grading the material composition near the interface decreases the height of the barrier. Adding doping pulses (typically, a sheet of Si donors) can also lead to a charge dipole (from the ionized Si dopants and compensating ionized acceptor dopants in the base) which can produce an electrostatic field to cancel the band offset contributions. A ‘setback’ layer of n-doped low bandgap material is also often introduced. A representative overall design, which has been used at UCSD to produce GaInNAs-based HBTs with base bandgap down to 1.0 eV, is shown in table 1 [6]. The design uses doping grading as well as pulse doping to eliminate the effects of conduction band barriers. The growth of this structure was undertaken with gas-source MBE. In order to decrease the difficulty of calibrating the growths of the graded materials at the interfaces, a chirped superlattice was employed, in which the material alternates between the end-point compositions (GaAs and GaInNAs) in a superlattice where the thickness of the two materials is progressively changed. In this example,

Table 1. Epitaxial layer design for GaInNAs HBT, incorporating provisions to overcome conduction band barriers at the BE and BC heterojunctions.

Layer	Material	Thickness (Å)	Doping (cm^{-3})
Cap	GaAs	2000	n 5×10^{18}
Emitter	GaAs	2000	n 5×10^{17}
Delta doping	GaAs	5	n 3×10^{19}
Graded	GaAs → $Ga_{0.89}In_{0.11}N_{0.02}As_{0.98}$	300	n 3×10^{17}
Spacer	$Ga_{0.89}In_{0.11}N_{0.02}As_{0.98}$	50	undoped
Base	$Ga_{0.89}In_{0.11}N_{0.02}As_{0.98}$	400	p 8×10^{18}
Spacer	$Ga_{0.89}In_{0.11}N_{0.02}As_{0.98}$	50	undoped
Graded	$Ga_{0.89}In_{0.11}N_{0.02}As_{0.98}$ → GaAs	300	n 3×10^{16}
‘Delta doping’	GaAs	50	n 1.5×10^{18}
Collector	GaAs	4000	n 3×10^{16}
Sub-collector	GaAs	7000	n 5×10^{18}
S.I. GaAs substrate			

the superlattice consisted of 15 periods, with a thickness of 11 Å per period. As detailed below, no effects of barriers were detected. In this example, the bandgap reduction in the base was sufficient that an emitter of GaAs could be used (rather than AlGaAs or GaInP) while still maintaining a large enough difference in bandgap between emitter and base to insure high electron injection efficiency; about 200–250 meV difference is needed to account for doping differences between base and emitter. The resulting band diagram is shown in figure 4(*b*). With MOCVD growth, the grading of composition is easier than in MBE, and a continuous grading is used. In most work a conventional AlGaAs or GaInP emitter layer is maintained, which allows the same processing to be used as for conventional HBTs, and facilitates passivation ledges, etch stop layers, etc.

In addition to the bandgap energy, other material characteristics are critical for high performance HBTs. The current gain of the device is influenced by the recombination lifetime of electrons in the base, as well as by the diffusion coefficient of electrons across the base. The component of base current associated with the base recombination, I_{br}, can be expressed as

$$I_{\mathrm{br}} = I_{\mathrm{C}}\, \tau_{\mathrm{btr}}/\tau_{\mathrm{rec}} \tag{4}$$

where I_{C} is the collector current, τ_{rec} is the recombination lifetime of electrons in the base, and τ_{btr} is the base transit time. For purely diffusion transport across the base (as obtained with uniform base doping and composition), τ_{btr} is given approximately by

$$\tau_{\mathrm{btr}} = w^2/2D_{\mathrm{n}} + w/v_{\mathrm{ex}}. \tag{5}$$

Here w is the base thickness, D_{n} is the electron diffusion coefficient, and v_{ex} is the average velocity at which electrons exit the base. The combination of the two above expressions shows that

$$I_{\mathrm{br}} = I_{\mathrm{C}}[(w/L_{\mathrm{diff}})^2/2 + w/v_{\mathrm{ex}}\tau_{\mathrm{rec}}], \tag{6}$$

where L_{diff} is the minority carrier diffusion length in the base. The contributions associated with v_{ex} become small for thick base layers or small diffusion lengths. Equation (6) illustrates that it is important to maintain a large value of diffusion length in the base ($L_{\mathrm{diff}} \sim 0.5$ (μm for a 500 Å GaAs base). It is noteworthy that the electrons which flow across the base have relatively low density ($<10^{16}\ \mathrm{cm}^{-3}$ typically) and thus occupy states at the very bottom of the conduction band, where they are particularly sensitive to band tailing effects, localization of states, etc. Other contributions to base current (including emitter-base recombination, emitter-edge recombination and hole injection into the emitter) must also be minimized.

To maintain high-frequency operation, the current gain cutoff frequency f_{T} must be high; $f_{\mathrm{T}} > 30$ GHz is desired in most applications. The value of f_{T} can be estimated through the relation,

$$\tau_{\mathrm{ec}} = \frac{1}{2\pi f_{\mathrm{T}}} = \tau_{\mathrm{btr}} + \tau_{\mathrm{CSCL}} + \frac{V_{\mathrm{T}}}{I_{\mathrm{C}}}(C_{\mathrm{BE}} + C_{\mathrm{BC}}) + C_{\mathrm{BC}}(R_{\mathrm{E}} + R_{\mathrm{C}}). \tag{7}$$

Here τ_{btr}, is the base transit time, τ_{CSCL} is the collector space-charge transit time, and the remaining terms are RC charging times associated with BE and BC depletion capacitances (C_{BE} and C_{BC}, respectively). The base layer influences f_{T} through the base transit time τ_{btr}, the same parameter that enters the current gain expression above. In conventional HBTs, τ_{btr} is about 1.2 ps, while the entire right-hand side of equation (7) is 4 ps. Thus by introducing a GaInNAs base, it is necessary to avoid increasing τ_{btr} by more than about 0.4 ps.

The microwave power gain of HBTs is specified by the figure of merit $f_{\max}$, the maximum frequency of oscillation, which can be calculated by the following equation,

$$f_{\max} = \sqrt{\frac{f_{\mathrm{T}}}{8\pi R_{\mathrm{B}} C_{\mathrm{BC}}}}. \tag{8}$$

To achieve high $f_{\max}$, it is necessary to have high f_T, as well as to maintain low base resistance, R_{B}. The value of R_{B} is directly influenced by the sheet resistance in the base, ρ_{B}, given by

$$\rho_{\mathrm{B}} = \frac{1}{qp\mu_{\mathrm{p}}w}. \tag{9}$$

The base must thus maintain high doping level, p, and high mobility for holes, μ_{p}; the sheet resistance ρ_{B} of 300–600 ohms/square achieved in conventional devices must not be increased significantly.

With the introduction of GaInNAs in the base in place of GaAs, the values of L_{diff} are found to decrease, which worsens the current gain, and the values of f_{T} drop. One strategy to mitigate these effects is to provide compositional grading across the base. By providing a change in bandgap of the base from a large value near the emitter (E_{gbe}) to a smaller value near the base-collector junction (E_{gbc}), a built-in quasi-electric field of value $\varepsilon_{\mathrm{b}} = (E_{\mathrm{gbe}} - E_{\mathrm{gbc}})/w$ can be designed into the device, so that electron flow proceeds by drift as well as by diffusion. Under such circumstances, the base transit time becomes

$$\tau_{\mathrm{btr}} = \frac{KTw}{qD\varepsilon_{\mathrm{b}}} + \left(\frac{1}{v_{\mathrm{ex}}} - \frac{KT}{qD\varepsilon_{\mathrm{b}}}\right)\frac{KT}{q\varepsilon_{\mathrm{b}}}\left(1 - \exp\left(\frac{-q\varepsilon_{\mathrm{b}}w}{KT}\right)\right). \qquad (10)$$

(This expression, evaluated within the drift-diffusion transport formalism, is valid only for small departures from equilibrium—and thus small values of $qD\varepsilon_{\mathrm{b}}/KT$ relative to v_{ex}). The built-in field is typically ~5–10 kV cm^{-1} or higher across a 500–1000 Å base, which can reduce the transit time by a significant factor.

3. Material growth and device processing

GaAs HBT epitaxial structures are currently produced in commercial quantities using both MBE and MOCVD techniques. Both approaches have been used by investigators to produce GaInNAs HBT structures. Work based on MOCVD typically employs dimethylhydrazine or ammonia as the nitrogen-containing species. For the MBE research to date, nitrogen was derived from a plasma source fed with N_2, within a gas-source MBE system (which provides the As in the form of AsH_3 fed into a suitable cracker). The acceptor dopant of choice for MOCVD growth is carbon; the acceptor of choice for MBE is beryllium (although carbon can also be used). The addition of In and N can lead to significant changes in growth rate and in dopant incorporation, so that extensive calibration is generally required.

It has been shown that the addition of N during growth changes the incorporation of hydrogen, which is prevalent in the growth ambient. The hydrogen has a significant role in compensating the acceptor dopants, so that the hole concentration is generally well below the acceptor impurity concentration incorporated. The hydrogen grown into the structure can be partially eliminated by annealing, which can be carried out during or after the growth. It is argued that a portion of the hydrogen exists (or migrates) as a positively charged entity, so that the evolution of hydrogen from the p-type base is impeded by the grown overlayer of n-type material (since the resulting p–n junction provides a built-in electric field which retards the motion). This suggests *in situ* annealing might be more worthwhile. However, it is possible that even after annealing, hydrogen could become incorporated during the subsequent growth of emitter and cap layers.

In the experimental work done to date on Be-doped, gas-source MBE-grown materials, annealing of the material subsequent to growth has been a key step. A principal effect is acceptor activation through hydrogen evolution; reduction of point defect concentrations can also take place. The anneal parameters must be carefully chosen, however, in order to avoid diffusion of the beryllium dopant incorporated in the base. Rapid thermal annealing (RTA) is the preferred process. Figure 5 shows the results of SIMS analyses showing the reduction of hydrogen content after RTA at 700 °C and at 850 °C for 10 s [7].

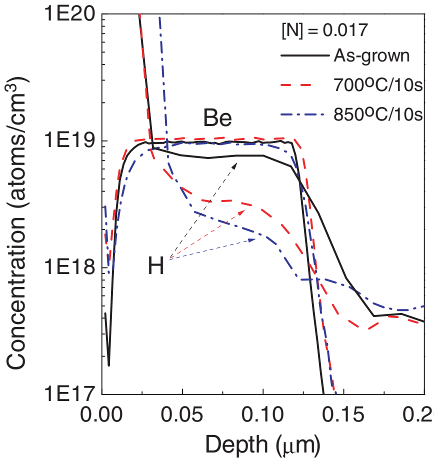

Figure 5. Profiles of Be and H measured by SIMS for a GaInNAs layer on GaAs, before and after rapid thermal anneals at 700 °C and 850 °C.

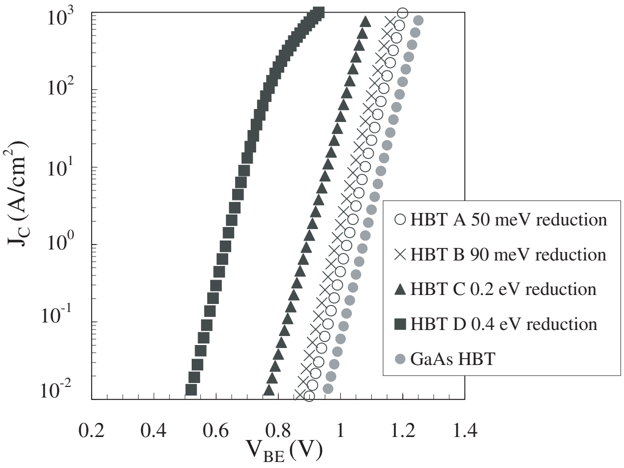

Figure 6. Collector current versus V_{be} for various experimental GaInNAs based HBTs, showing reduction in V_{be}.

Processing of HBTs employing GaInNAs bases is largely identical to that employed for conventional GaAs base layers. However, formation of ohmic contacts to the base is more difficult if the base doping is low. If an emitter of GaAs is used in place of GaInP or AlGaAs, then it is difficult to use selective etching that stops accurately at the base layer, since it appears that the GaInNAs etches at least as rapidly as GaAs in wet chemical etches. A process simplification when etching down to the base layer is to use plasma etching with a chlorinated gas such as CCL_2F_2 which has been reported to stop on indium containing materials [8, 9]. However, there is a concern that plasma etching may degrade the material quality.

4. Experimental results

HBTs with GaInNAs base regions have been demonstrated by numerous investigators, with varying amounts of N and In [6, 10–15]. Several devices are described in the following, to provide a representative picture of the results obtained.

GaInNAs HBT device characteristics exhibit the expected reduction in $V_{\mathrm{be,on}}$, as demonstrated in figure 6. This figure shows curves of J_C versus V_{be} measured for several reported GaInNAs HBTs, and a conventional HBT with GaAs base for

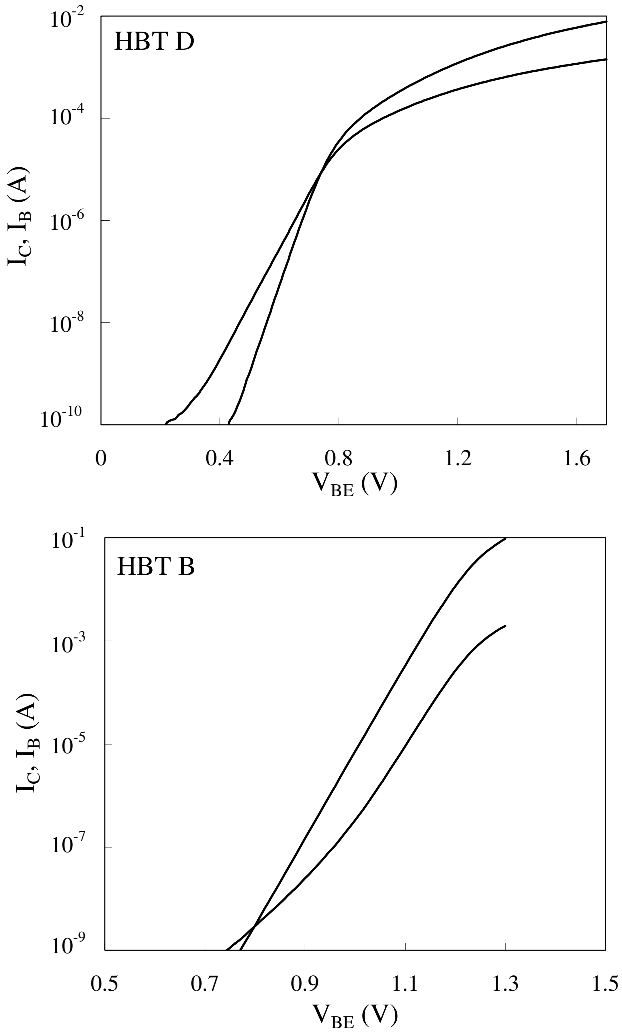

Figure 7. Gummel plots measured for GaInNAs HBTs of type B and type D.

comparison. GaInNAs HBT A and B were grown by Kopin using MOCVD; HBT A has a reduction in $V_{\mathrm{be,on}}$ of 50 meV [10] while B has a 90 meV reduction [11]. These devices employ relatively low values of In and N in order to maintain high current gain and low base sheet resistance. GaInNAs HBT C shows a 0.2 eV reduction in $V_{\mathrm{be,on}}$ and was grown at Emcore by MOCVD [12]. GaInNAs HBT D was grown at UCSD via gas-source MBE using 2% N and 11% In, to produce a large change in $V_{\mathrm{be,on}}$; an observed $V_{\mathrm{be,on}}$ reduction of 0.4 eV was demonstrated [6].

The base current corresponding to devices B and D is evident in figure 7, which shows the full Gummel plots for the devices (log I_C and log I_B versus V_{be}, for $V_{BC} = 0$). The characteristics of device D show relatively large curvature at high currents due to base series resistance effects. In figure 8, common-emitter I_C versus V_{CE} curves are also shown. The curves indicate that the base current increases with increasing N and In content. The curves of I_B versus V_{be} are characterized by ideality factors near unity, so that recombination in the base is a predominant source of base current (although for device D the recombination in the emitter-base junction is also likely to be important). The decrease in current gain allows a simple estimate of the diffusion length in the GaInNAs base. Following equation (6), L_{diff} is estimated to be of the order of 0.4 μm for device B (550 Å base) and of the order of 0.1 μm in device D (400 Å base). Diffusion length is a material parameter that typically depends strongly on the material preparation technique, as well as on the acceptor doping, and in GaInNAs, on the N concentration. The value of L_{diff} for sample B shows that even for a small amount of N concentration, the transport of electrons through the base is degraded. The diffusion length for a 500 Å p^+ GaAs is 0.5 μm. The value of L_{diff} for sample D, which has $p \sim 8 \times 10^{18}$ cm^{-3}, is significantly lower than would be obtained in GaAs of comparable doping, and is presumably limited by reduced electron mobility in GaInNAs, as well as by enhanced recombination.

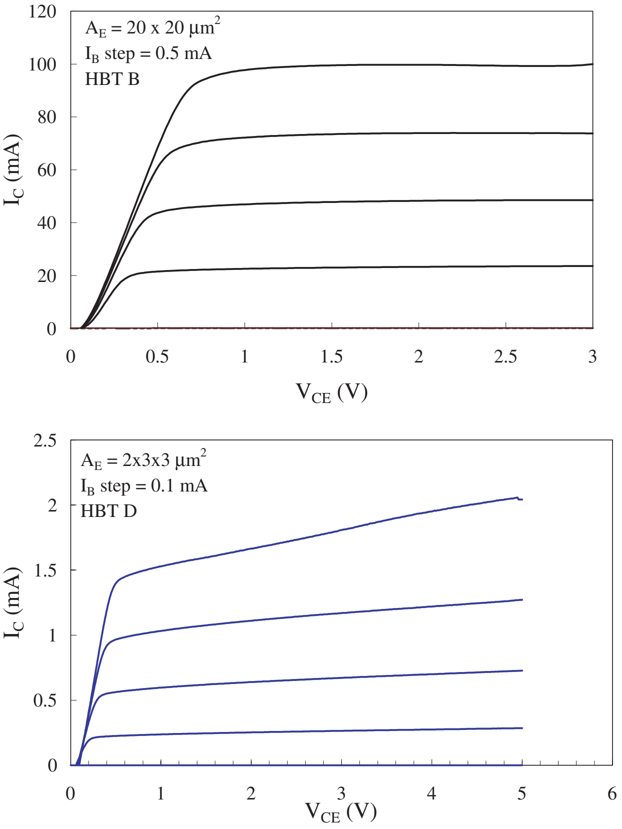

Figure 8. Experimental I_C–V_{CE} curves obtained for GaInNAs HBTs type B and type D.

An interesting feature that has been determined for GaInNAs base HBTs is the temperature dependence of current gain. For conventional HBTs the current gain typically decreases with increasing temperature T, as a result of higher injection of holes to the emitter, higher space charge layer recombination current, and possible shorter diffusion length in the base. In the GaInNAs device D, a significant increase in current gain is found with increasing T (0.3% increase for each one-degree temperature rise, which corresponds with an ‘activation energy’ in an Arrhenius plot of 40 meV). This result is interpreted as an increase in diffusion length with increasing temperature. Such an effect would be expected if electrons at the bottom of the band are confined in states that are at least partially localized, and with increasing temperature they are

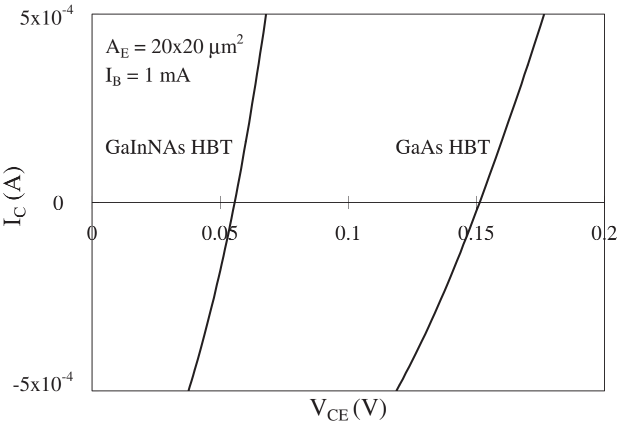

Figure 9. Measured values of I_C versus V_{CE} for a GaInNAs HBT (type B) and a reference HBT with GaAs base, showing the offset voltage reduction obtained.

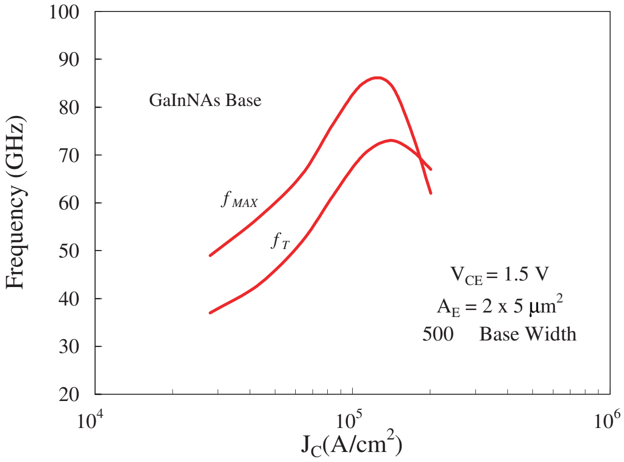

Figure 10. Experimental values of f_T and f_{max} as a function of current density obtained for GaInNAs HBT (type A).

thermally excited out of those states to others in which the electrons can diffuse more readily.

The base sheet resistance achieved differs significantly among growths. For device B, base sheet resistance is 500 ohms/square, while for device D it is 7000 ohms/square (as evaluated by transmission line method measurements on test patterns incorporated on the same wafer as the HBTs). The strong increase in base resistance in device D is presumed to be the result of hydrogen passivation of the beryllium acceptors, that is only incompletely removed by the rapid thermal anneal process (as well as by a lower acceptor incorporation, $[\mathrm{Be}] = 8\times10^{18}$ cm^{-3} versus $[\mathrm{C}] = 3\times10^{19}$ cm^{-3} in device B).

In the common-emitter *I*–*V* curves of figure 8, negative output conductance is observed for device B. This feature is commonplace in conventional HBTs with GaAs bases, as a result of self-heating effects. By contrast, in device D there is a prominent positive output conductance. This effect can be explained in detail by the depletion of holes in the base from the application of collector bias V_{CE} (the associated increase in I_C can be calculated from equation (1)). This effect is significant in device D because of the lower base sheet doping.

The shape of the *I*–*V* curves suggests that any energy barriers in the conduction band have been adequately minimized by the techniques used. For device B, this consisted of grading of the material composition during MOCVD growth, while for the MBE-grown sample D, it was the result of a chirped-superlattice grading together with delta-doping, as mentioned in section 2.

Inspection of the I_C–V_{CE} curves of device B indicates a change in the characteristics in the vicinity of $I_C = 0$. This region is shown magnified in figure 9, and, for comparison, the characteristics of a representative HBT with GaAs base. The value of I_C goes from negative values at low bias to positive values only when V_{CE} exceeds a critical amount, termed the offset voltage V_{offset}. For the GaAs device, V_{offset} is of the order of 0.15 V (and for other related devices can be up to 0.25 V). It is desirable to reduce this voltage for most circuit applications, particularly for high-efficiency power amplifiers. Figure 9 illustrates that V_{offset} is lower for the transistor with GaInNAs base material. This result can be understood on the basis of the base-collector junction structure in the two devices. In the GaAs device, both base and collector consist of GaAs, and under forward bias conditions, the current flow can take place by both electrons and holes. Because of the asymmetric doping ($\times10^3$ higher in the base than in the collector) holes are largely responsible for the current. The BC junction voltage is thus smaller than the BE heterojunction voltage for a given amount of current flow, and the difference translates into the offset voltage. In the GaInNAs device, the bandgap of the base is smaller than that of the collector (GaAs), and so the hole current is substantially blocked by the valence band barrier between the two materials (which occurs in the same way as hole current blocking by a wide bandgap emitter). As a result, the turn-on voltage for the BC junction is very similar to that of the BE junction, and the offset voltage is minimized.

Microwave measurements have been made on a number of the GaInNAs devices. These measurements require fabrication of devices with relatively small dimensions (emitter width below 5 μm) inasmuch as at high frequency and high current density there is a tendency for current density to ‘crowd’ at the edges of the emitter, and large area devices are not uniformly excited. Figure 10 shows the measured variation of f_T and f_{max} with current density for a device of type A with 2 μm $\times$ 5 μm emitters. The results indicate that there is a small decrease in f_T, from 78 GHz to 73 GHz, as a result of the GaInNAs base. If the reduction in f_T, is attributed entirely to a larger value of base transit time, then the transit time increase is calculated to be 0.14 ps. This modest increase can be expected for a change in minority carrier mobility of order 10%. Similar measurements have been done for a device of type D. In this case the peak f_T drops to a value of 23 GHz, at lower than usual J_C of 2.6×10^4 A cm^{-2}, due to large emitter parasitic resistance in this particular device. The results correspond to an increase of base transit time to 2 ps. An increase of this magnitude would require an electron diffusion coefficient of 6 (lower than that of GaAs by a factor of 3–5).

A summary of the results of various GaInNAs HBTs reported in the literature is provided schematically in figure 11. Here the current gain achieved is plotted versus the reduction in $V_{be,on}$ relative to GaAs. The base sheet conductivity reported for the devices is also shown. The results clearly indicate that the benefit of lower $V_{be.on}$ must be obtained at the cost of worse performance in other parameters.

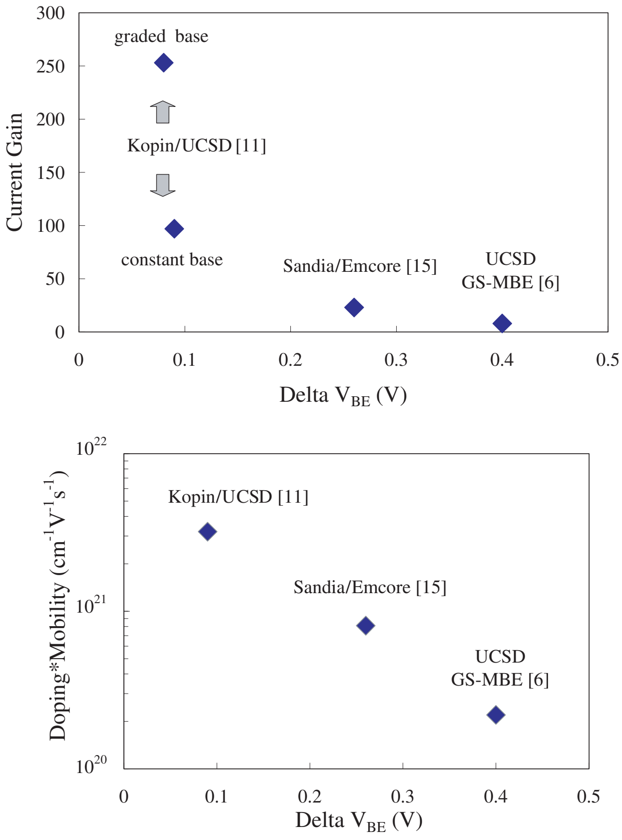

Figure 11. Plots of current gain versus V_{be} shift from GaAs HBTs obtained for various reported GaInNAs based HBTs; also shown is the base sheet conductivity versus V_{be} shift for these devices.

Compositional grading within the base layer is a design approach intended to minimize the unfavourable effects of GaInNAs bases, as described in section 2. Initial demonstrations of such devices have already been undertaken [11]. Using MOCVD, HBTs were grown with base regions of thickness 550 Å and 3×10^{19} cm^{-3} carbon doping level (together with appropriate spacers to remove conduction band barriers). The GaInNAs composition was graded to provide built-in quasi-electric fields of the order of 9 kV cm^{-1}. The devices showed the expected reduction of V_{be} of 80 meV, while the current gain of the transistor was improved from that of a device with GaAs base fabricated at the same time. The corresponding current gain experimental results are shown in figure 12. RF measurements were subsequently carried out on the devices, which showed that the GaInNAs transistor with graded composition base had performance equivalent to that of the GaAs control HBT (with peak f_T of 63 GHz at $J_C = 10^5$ A cm^{-2}). These results suggest that the effects of reduced electron mobility in GaInNAs can be completely overcome with compositionally graded bases.

Most of the reported efforts to fabricate HBTs with GaInNAs bases have focused on npn devices, which are faster than pnps and are the only devices in current production. Work by Hou *et al* has also shown that GaInNAs bases are advantageous for pnps. For these devices, the change in conduction band energy (and small change in valence band energy) is favourable for minority carrier confinement in the base, without worry about the need for compositional grading.

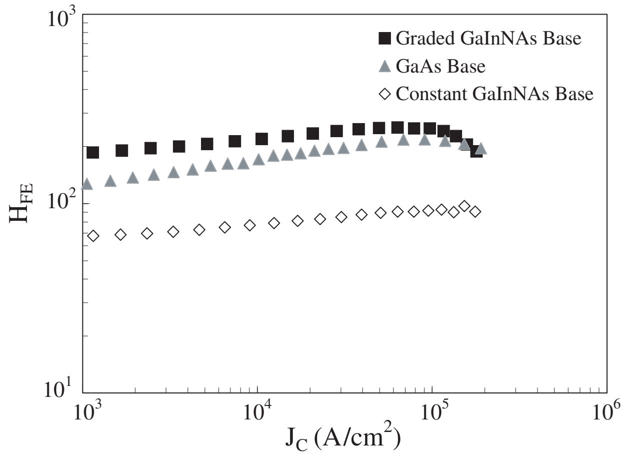

Figure 12. Experimental results of current gain versus collector current density for a conventional GaAs base HBT, and GaInNAs base HBTs with constant and graded alloy composition.

Also the prospect of using p-type GaAs (rather than GaInP or AlGaAs) in the emitter and collector layers is attractive. Reported devices had $V_{be,on}$ reduction of 290 meV, current gain as high as 60, and f_T of 15 GHz [14].

5. Future outlook

The incorporation of GaInNAs in the base of HBTs is a scientifically interesting and commercially important addition to the material and bandgap engineering capabilities for III–V compound devices. An advantage of this approach is that structures can be produced with very small deviations from current production standards, which significantly reduces the barriers to introduce the technology into products. For the case of HBTs, there is considerable benefit to be gained from relatively small reductions in $V_{be,on}$, because of the particular voltages now in use for battery-operated circuits. If much more dramatic reductions in $V_{be,on}$ are required, it is likely that a large change in structure, such as using InGaAs bases on InP substrates, will become the favoured approach.

HBTs on GaAs substrates with base regions of GaAsSb have also been suggested to provide a lower turn-on voltage than HBTs with GaAs bases [16]. The GaInNAs material system for the base is potentially more flexible than GaAsSb, because it provides the ability to maintain lattice match to the substrate even with substantial change in bandgap.

Initial laboratory demonstrations have shown that for N concentration over a limited range and for graded composition base layers, high performance devices can be produced. A major task for the future is to verify that the reliability of the resulting devices can be high enough to meet the exacting requirements of the marketplace. HBT reliability is known to be strongly dependent on the material quality. While initial measurements with GaInNAs have not revealed any significant reliability issue, much work remains to be done. In the most favourable scenario, the lower bandgap energy of GaInNAs may lead to lower recombination-enhanced defect motion, which would in principle make the GaInNAs devices even more reliable than conventional devices [17].

Acknowledgments

The authors are grateful to Kazuhiro Mochizuki, Peter Zampardi, Richard Pierson, James Li, Hong Hou, Nelson Li, Tatsuo Itoh and Frank Chang for many helpful discussions, and for the efforts of the entire Wafer Engineering Group at Kopin Corporation. Funding support from the ARO under the MURI Low Power and Low Noise Electronics for Wireless Communications, and from Rockwell Scientific, and from the Air Force Research Laboratory, Sensors Directorate (STTR funding contract no F33615-99-C-1510) is gratefully acknowledged.

References

[1] Miyamoto T, Takeuchi K, Kageyama T, Koyama F and Iga K 1999 Chemical beam epitaxy of GaInNAs/GaAs quantum wells and its optical absorption property *J. Cryst. Growth* **197** 67

[2] Tournie E, Pinault M-A, Vezian S, Massies J and Tottereau O 2000 Long wavelength GaInNAs/GaAs quantum-well heterostructures grown by solid-source molecular-beam epitaxy *Appl. Phys. Lett.* 2189

[3] Kondow M, Kitatani T, Nakatsuka S, Larson M C, Nakahara K, Yazawa Y, Okai M and Uomi K 1997 GaInNAs: a novel material for long-wavelength semiconductor lasers *IEEE J. Sel. Top. Quantum Electron.* **3** 719

[4] Xin H P and Tu C W 1998 GaInNAs/GaAs multiple quantum wells grown by gas-source molecular beam epitaxy *Appl. Phys. Lett.* **72** 2442

[5] Niki S, Lin C L, Chang W S C and Wieder H H 1989 Band-edge discontinuities of strained-layer $In_xGa_{1-x}As$/GaAs heterojunctions and quantum wells *Appl. Phys. Lett.* **55** 1339

[6] Welty R J, Xin H P, Mochizuki K, Tu C W and Asbeck P M 2002 GaAs/$Ga_{0.89}In_{0.11}$ $N_{0.02}As_{0.98}$/GaAs NpN double heterojunction bipolar transistors with low turn-on voltage *Solid-State Electron.* **46** 1

[7] Xin H P, Kavanagh K L and Tu C W 2000 Gas-source molecular beam epitaxial growth and thermal annealing of GaInNAs/GaAs quantum wells *J. Cryst. Growth* **208** 145

[8] Cooper C B III, Salimian S and MacMillan H F 1987 Use of thin AlGaAs and InGaAs stop-etch layers for reactive ion etch processing of III-V compound semiconductor devices *Appl. Phys. Lett.* **51** 2225

[9] Seaward K L, Moll N J, Coulman D J and Stickle W F 1987 An analytical study of etch and etch-stop reactions for GaAs on AlGaAs in CCl_2F_2 plasma *J. Appl. Phys.* **61** 2358

[10] Welser R E *et al* 2001 Pathway for HBT turn-on voltage reduction on a GaAs platform *Int. Conf. Gallium-Arsenide Manufacturing (Las Vegas, NV)* p 30

[11] Welser R E and Welty R J to be published

[12] Chang P C, Baca A G, Li N Y, Sharps P R, Hou H Q, Laroche J R and Ren F 2000 InGaAsN/AlGaAs P-n-p heterojunction bipolar transistor *Appl. Phys. Lett.* **76** p 2788

[13] Welser R E, DeLuca P M and Pan N 2000 Turn-on voltage investigation of GaAs-based bipolar transistors with GaInAsN base layers *IEEE Electron Device Lett.* **21** p 554

[14] Monier C, Baca A G, Chang P C, Li N Y, Hou H Q, Ren F and Pearton S J 2001 Pnp InGaAsN-based HBT with graded base doping *Electronics Lett.* **37** 198

[15] Monier C, Baca A G, Chang P C, Newman F, Li N Y, Armour E, Briggs R D and Hou H Q 2001 High-speed performance of NpN InGaAsN-based double heterojunction bipolar transistors *State-of-the-Art Program on Compound Semiconductors (Electrochemical Society Proceedings) (San Francisco, CA)* p 62

[16] Oka T, Mishima T and Kudo M 2001 Low turn-on voltage GaAs heterojunction bipolar transistors with a pseudomorphic GaAsSb base *Appl. Phys. Lett.* **78** 483–5

[17] Welser R E and DeLuca P M 2001 Exploring physical mechanisms for sudden beta degradation in GaAs-based HBTs *Proc. GaAs Reliability Workshop* p 135